Enhancing the recovery of cement-rich powder from recycled fine aggregates through thermal shock

Gebremariam, Abraham T.; Vahidi, Ali; Di Maio, Francesco; Chang, Cheng; Rem, Peter

DOI
10.1016/j.cscm.2025.e05272

Publication date
2025

Document Version
Final published version

Published in
Case Studies in Construction Materials

Citation (APA)
Gebremariam, A. T., Vahidi, A., Di Maio, F., Chang, C., & Rem, P. (2025). Enhancing the recovery of cement-rich powder from recycled fine aggregates through thermal shock. *Case Studies in Construction Materials*, *23*, Article e05272. https://doi.org/10.1016/j.cscm.2025.e05272

Case Studies in Construction Materials 23 (2025) e05272

Contents lists available at ScienceDirect

Case Studies in Construction Materials

journal homepage: www.elsevier.com/locate/cscm

Enhancing the recovery of cement-rich powder from recycled fine aggregates through thermal shock

Abraham T. Gebremariam [*], Ali Vahidi, Francesco Di Maio, Cheng Chang, Peter Rem

Department of Engineering Structures, Faculty of Civil Engineering and Geosciences, Delft University of Technology, Delft, the Netherlands

ARTICLE INFO

Key words:
Recycled cement rich Powder
Recycled fine aggregates
Spalling
Thermal treatment
Recycling

ABSTRACT

This study presents a method for recovering cement-rich powder from recycled fine aggregates by thermal shock, during which particles are fragmented and spalled due to differential thermal stress. When recycled fine aggregates (RFA) are exposed to high temperatures, the cement paste-rich boundary between the aggregates is weakened and spalled, liberating cement rich particles due to thermal shock. To investigate this phenomenon, experiments have been carried out by subjecting fine recycled aggregates to high temperatures ranging from 500 °C to 700 °C at different residence times. The result suggests that the particles split and crackle due to thermo-mechanical changes. Following thermal treatment, gentle milling completes the liberation process of recycled cement-rich powder (RCP). The composition of the recovered powder confirms the feasibility of the recovery method. To understand the thermo-mechanical process better, modelling efforts have been carried out on a spherical concrete particle of known diameter. The model predicts the temperature profile, residence time and radial stress inside the particle. According to the model, a 2 mm particle experiences a radial stress high enough to overcome the tensile strength of the concrete within 35 s, causing cracks due to the thermal gradient created between the inner and outer surfaces of the particle. These predictions have been verified by experimental results in the laboratory. This approach not only enhances recovery of RCP but also promotes sustainable construction practices.

1. Introduction

Recycling of concrete is gaining more attention not only due to the environmental concerns related to generating and accumulating concrete waste but also due to its enormous potential as a source of raw materials for the construction sector. Nowadays, the use of recycled coarse aggregates is practiced widely to produce sustainable concrete [1–3]. Consequently, recycling concrete facilities existing today aim to crush and sell the coarse aggregate fraction. Nevertheless, only a little effort is made to recycle or upcycle the fine fraction [4,5]. This is due to the fact that Recycled Fine Aggregates (RFA) are composed of mortar and other contaminants that require extra effort to separate cement paste from aggregate surface. These problems, added to the lack of technologies and market, make their application less practical for concrete structures. As a result, their application has been limited to road base aggregates or land filling [6,7]. Indeed, addressing such a complex problem necessitates careful research, technological advancement, and collaboration between researchers, industry stakeholders, and policymakers. Understanding and tackling these challenges would help to develop

---

[*] Corresponding author.
E-mail address: a.t.gebremariam@tudelft.nl (A.T. Gebremariam).

https://doi.org/10.1016/j.cscm.2025.e05272
Received 18 June 2025; Received in revised form 19 August 2025; Accepted 4 September 2025

efficient recycling processes and promote the widespread use of RFA. This does not only mitigate the environmental issues related to concrete wastes but also provide a solution to the prevailing sand [8,9].

Globally, there is a consensus on the need to recycle End-of-Life (EoL) concrete wastes into high-quality raw materials because this helps to implement an economic model based on circular use of building materials. Now that the construction sector is under constant pressure towards sustainable construction practices, several measures have been introduced to urge the sector to find sustainable alternative resources that originate from construction and demolition activities. For instance, in the Netherlands, there are clear ambitions set by the "concrete agreement (BETONAKKOORD)" which states that 100 % of all concrete residual flows will be recycled at a quality level that can be used by 2030 in such a way that it can be permanently applied in new concrete [10]. This highlights the amount of effort necessary to build sustainable technologies beyond laboratory scale to recycle the fine fraction of aggregates and replace the already depleting natural sand [8]. This ambition has created some innovation in recycling and processing of secondary raw materials from EoL concrete, [11–14]. Most of which are based on thermal and mechanical methods where the aggregates are exposed to elevated temperature to weaken the adhered mortar that can be easily removed mechanically by milling [15–17]. Thermo-mechanical activation of recycled cement powder typically involves controlled thermal treatment (∼450–900 °C) followed by mechanical milling to enhance reactivity and repurpose it as a supplementary cementitious material. Some studies report that there is an optimal thermal window between 400 and 750 °[18,19]. Thermally activated RCP shows significantly improved mortar performance—enhanced compressive strength and denser microstructure—compared to unmodified [20,21]. The improvements stem from the breakdown of hydration products (e.g., C–S–H), which form more reactive, partially dehydrated phases. According to Fu et al. [22], the cracking of concrete upon heating is caused by an incompatibility of thermal expansion of the aggregate and the cement paste, resulting in high traction stresses in the inter-phase transition zones and the development of local micro-cracks. Gawin et al. [23] also studied that the strength loss of concrete with temperature is attributed to cracks that appear during chemical transformations of concrete during dehydration and decomposition of phases. Mechanical grinding post-thermal treatment increases specific surface area and particle reactivity, further aiding hydration kinetics and densification [18,21,24]. Thus, thermo-mechanical activation represents a promising route for valorizing RCP into viable low-carbon binders.

Although thermo-mechanical recycling methods improve aggregate quality through the liberation of mortar from the aggregate surface, they have notable disadvantages. These include high energy consumption, increased CO_2 emissions, and equipment wear, making the process environmentally and economically expensive [25]. The challenge lies in finding an economical method to recycle fine aggregates that preserves the integrity of the recycled sand while simultaneously recovering the cement-rich powder. Thus, thermal shock–based methods could offer several advantages over conventional soak-based thermo-mechanical methods that require prolonged high-temperature exposure [5,18,26]. Thermal shock relies on rapid heating to induce internal stresses that selectively crack the aggregate–paste interface. This approach is faster, more energy-efficient, and results in lower CO_2 emissions, since it avoids long furnace cycles.

The effect of thermal shock on the cement paste matrix, however, is not clearly understood. According to Alonso et al.[27], CSH starts decomposing at temperatures as low as 100–250°C and the rate of decomposition dramatically increases after 560°C [28]. The cracks, the pore pressure, shrinkage, and other phenomena observed when concrete is exposed to high temperatures are indications of the weakening of the cement matrix in one form or another. Recycling large concrete chunks by heating to high temperatures may not be economical, as the cost of energy often outweighs the final aggregate value. Instead, it is advisable to separate the fine fraction (0–4 mm) where most of the hydrated cement phase is attached to and then expose to thermal shock for a short period of time. This approach is considered viable due to its practicality to thermally treat fine particles within shorter residence times, thereby enhancing energy efficiency. The approach, however, requires creating sufficient thermal gradient and stress to liberate the particles that have been glued together by cement but not so high that the internal stress breaks the silicate grains.

1.1. Research significance

The recycling of concrete remains an active area of research, primarily due to the challenges associated with effectively recovering the cement-rich powder from both the coarse and fine recycled aggregate fractions. Studies have shown that recycled coarse aggregates typically retain approximately 20–40 % of adhered mortar, whereas the fine fraction, comprising particles smaller than 4 mm, can contain up to 55 % or more of residual cementitious material [29,30]. Although the reuse of recycled aggregates supports resource efficiency and promotes circular economy principles in the construction sector, the carbon footprint could be significantly improved by

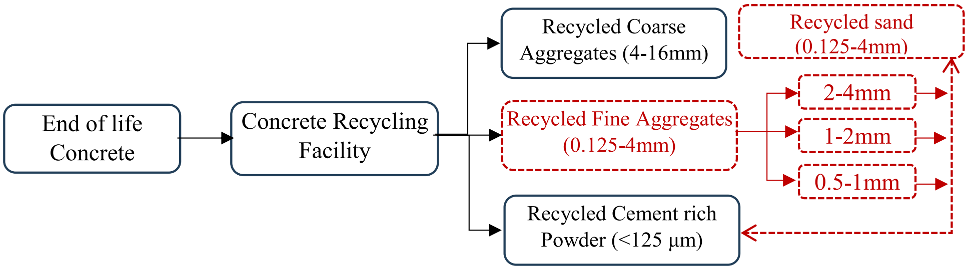

Fig. 1. Flow chart of the research scope highlighting the targeted processing and separation steps (shown in red broken lines).

maximizing the recovery of the cement-rich fraction. This is especially important given that cement production accounts for a substantial share of global CO_2 emissions. In this context, the present study focuses on the recovery of cement-rich powder from the fine fraction of crushed concrete that comprises most of the remaining cement paste. The methodological approach and research scope are illustrated in the flow chart presented in Fig. 1, highlighting the targeted processing and separation steps aimed at optimizing the recovery of this valuable material.

The subject of this study is, therefore, to examine the right process variables used to liberate and recover cement paste-rich powder from the fine fraction of recycled aggregates through thermal shock. When fine recycled aggregates are introduced to high temperatures, the surface of the concrete begins to expand, but the interior of the concrete remains relatively cool and that drives the particle to weaken and form micro-cracks. This process can be exacerbated by the presence of moisture within the concrete, which can cause the water to expand rapidly when heated and contribute to the cracking and spalling. By optimizing the temperature and exposure time, it is possible to make good use of controlled spalling to liberate RCP from RFA. Under controlled residence time and temperature, the degree of crackling and spalling is studied by exposing RFA particles to different temperatures, followed by milling. The intention of this study lies in maximizing RCP yield and not enhancing its reactivity. Furthermore, 1D model has been developed to understand the process by mimicking similar conditions that may cause thermal shock. The model is verified by experiments carried out under controlled conditions in an oven.

2. Experiments, material and methods

2.1. Baseline study

In this study, three distinct RFA particle sizes are prepared by sieving, namely, 2–4 mm, 1–2 mm and 0.5–1 mm. Initial properties of each size class are studied prior to being exposed to thermal shock. These particles are treated in 4 N HCl for a couple of hours [31, 32]. Once the acid reacts with the cement paste matrix, it is decanted and washed with distilled water until neutral pH. The contents are then filtered using Whatman filter paper (Φ100 mm). After drying the solid particles retained on the filter paper, the Particle Size Distribution (PSD) is determined by sieving. An optical microscopic image of recycled sand grains is used to compare the morphology before and after acid washing. The PSD of samples examined at this stage is regarded as a baseline property and is later compared with the PSD of heat-treated aggregates.

2.2. Thermal treatment of RFA

These experiments are carried out by placing a steel box of thickness 100 μm inside an oven set at 600 °C. Once the oven temperature reaches a stable reading, particles are placed inside the steel box and then the steel box is quickly placed into an oven. After a specific residence time of 15, 25, 35 and 40 s, the box is removed from the oven, and particles are collected into a container for subsequent analysis. The process is repeated until enough sample is collected for further study. The temperature of interest is 600 °C-700 °C. The temperature inside the steel box is monitored with an IR thermometer as shown in Fig. 2. The products are further analyzed to examine the liberation/breakdown of particles. In this experiment, the conditions are better defined and are used to validate the model.

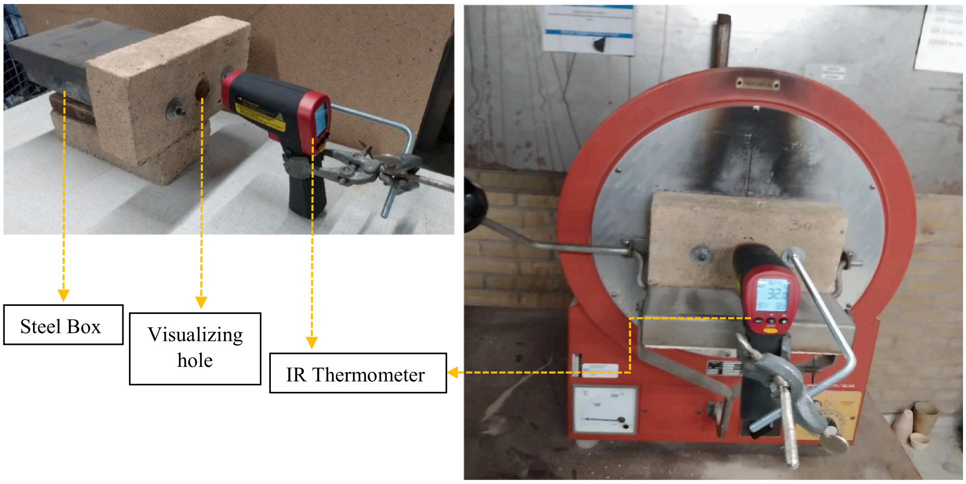

Fig. 2. Experimental setup for experiments in an oven along with an IR thermometer to measure the temperature inside the steel box.

2.3. Milling experiments

Milling experiments are carried out after the particles have been subjected to thermal treatment. The main intention of this experiment is to further liberate cement paste particles that have been weakened by spalling. For this purpose, 8–12 mm steel balls are used inside a horizontally rotating cylinder. The mass proportion of balls to sample is 5:1. Milling has been conducted for 5, 3, 2 and 1 min with the intention of optimizing the milling time.

2.4. Composition of RFA (CaO/SiO2)

This experiment aims to understand the role of thermal treatment in liberating cement paste from RFA by monitoring the composition of each particle size before and after thermal treatment. Since CaO and SiO_2 are the major cement components, tracking these values can give evidence about the changes in composition before and after thermal treatment. To this end, the composition of the fine aggregates is determined by pulverizing each sample into powdered form and analyzing by XRF (PANalystical, epsilon3-XL). Similarly, the composition of thermally treated particles is determined by sieving and pulverizing the particles retained on each sieve. A disc mill is used to pulverize particles into powders of particle size less than 125 μm. The composition of each sample is determined with XRF, and this is used to monitor the variations in the amount of CaO or SiO_2 after each process. In general, the trend in composition gives vital information about the amount of CaO and SiO_2 along with each particle size.

2.5. Performance of RCP in mortar

This study aims to assess the reusability of RCP by partially substituting cement at 10 %, 15 %, and 20 % replacement rates in a mortar. A control mix (Ref) and three experimental mixes are prepared using a fixed sand-to-binder ratio (3:1), by adjusting the slump within the range of 110–130 mm. The consistency of the mortar is performed according to NEN-EN 1015–3. CEMIII has been used as a binder. Mortar prisms (40 mm x 40 mm x 160 mm) are cast and cured under controlled conditions in a curing room ($\geq$95 % RH, 20 $\pm$ 2°C). Four prism samples are prepared, namely Ref, RCP_10, RCP_15 and RCP_20 that contain 0 %, 10 %, 15 % and 20 % RCP, respectively. The mix design is shown in Table 1. The prisms are tested for compressive strength at 2, 14, and 28 days per EN 196–1, with three replicates per mix. This data will help to compare strength development over time and determine the optimal RCP substitution rate without compromising the performance.

2.6. Modelling study

Several experimental and numerical studies have investigated spalling mechanisms [2,3], but simplified predictive models remain valuable for engineering applications. This work develops a numerical model that couples heat transfer and stress development to predict crackling in a concrete particle. For this, a 1D model is proposed to better understand the behavior of a concrete particle in a hot surrounding. The model is built to estimate the thermal stress within the concrete particle, when the particle surface is exposed to higher temperatures. A moist and microporous spherical concrete particle of moisture content 6 % by weight is assumed for this study. The particle is exposed to hot surroundings, as shown in Fig. 3.

As a crude (conceptual) model, some assumptions are made during the development of the model. Some of these are discussed below:

1. The moist particle first heats up due to the transfer of heat by convection and radiation, to a temperature of $T_b \cong 100$ °C, at which the internal moisture starts to vaporize and expand.
2. Then, in a second phase, the moisture inside the particle boils away from an internal boundary $r = R_m(t)$ between the moist inner part $0 < r < R_m$ (light grey) and the dry outer part $R_m < r < R$ (white) of the particle.
3. In the second phase, the heat delivered to the particle is primarily used to evaporate the moisture, i.e., only a small, insignificant part is used for heating up the dry outer part and the escaping water vapor to temperatures higher than T_b. In this phase, the pressure inside the particle remains approximately atmospheric and the boiling temperature is roughly $T_b = 100$ °C.
4. In a third phase, the dry particle surface is heated to higher temperatures, bounded by the temperature of the heating media.

The above conditions are satisfied for small particles ($<$ 4 mm) that are heated fast but not so fast that extreme gradients develop inside the particle. This is an interesting regime, since the application requires sufficient gradients and stress to liberate the cement paste, but not so high that the internal stress destroys the silicate grains themselves. In addition, it is the aim to keep the overall

Table 1
The composition of mortar mix design.

Sample	CEM III	RCP	Sand	Water
Reference	450 g	0 g	1350 g	225 g
RCP_10	405 g	45 g	1350 g	236 g
RCP_15	382.5 g	67.5 g	1350 g	245 g
RCP_20	360 g	90 g	1350 g	252 g

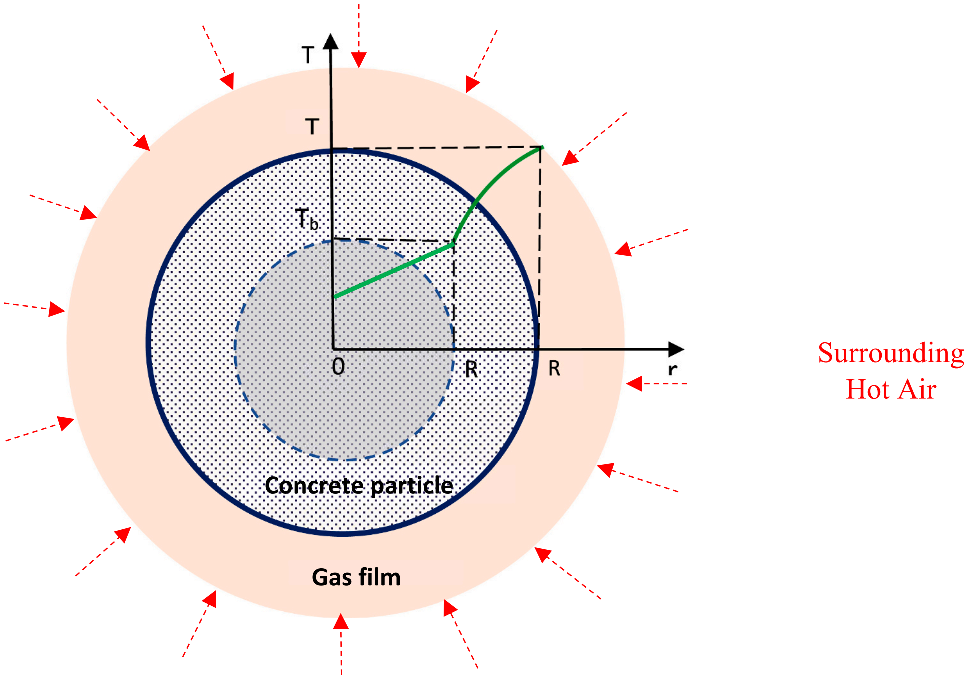

Fig. 3. Temperature distribution in a moist particle exposed to a hot surrounding (conceptual model).

(average) temperature (and surface temperature T_s) of the particles as low as possible to minimize energy consumption.

The governing equation for the transient heat transfer equation in a spherical coordinate given as:

$$\frac{\partial T}{\partial t} = D\left(\frac{\partial^2 T}{\partial r^2} + \frac{2}{r}\frac{\partial T}{\partial r}\right) \tag{1}$$

Where, T is the temperature, t is time, r is the radial position, and D is the thermal diffusivity. Boundary conditions include, at surface (r = R): $-k\frac{\partial T}{\partial t}|_{r=R} = h(T_\infty - T(R,t)) + \sigma\epsilon\left(T_\infty^4 - T_s^4\right)$ and at centre (r = 0): $\frac{\partial T}{\partial t}|_{r=0} = 0$ [33]. Where h is the convective heat transfer coefficient (W/m^2·K), σ is Stefan-Boltzmann constant, ϵ is emissivity, T_∞ is the ambient temperature (600°C).

The above equation is solved numerically using finite difference methods, with appropriate time-stepping to capture rapid temperature changes. With the above conditions, at time t, a temperature profile $T(r,t),\ 0 < r < R$ inside the particle is dictated by the moist boundary radius $r = R_m(t)[\mathrm{m}]$ and the rate of heating the particle surface $Q(t)[\mathrm{W}]$:

$$T(r,t) = \begin{cases} T_b & 0 < r < R_m \\ T_b + \dfrac{Q(t)}{4\pi\lambda_c}\left(\dfrac{1}{R_m(t)} - \dfrac{1}{r}\right) & R_m < r < R \end{cases} \tag{2}$$

According to Fourier's law [34], the heat flux $Q(t) = 4\pi r^2\lambda_c\frac{\partial T}{\partial r}$ for all $R_m < r < R$ within the approximation. Here, $\lambda_c \cong 1.2$ W/m℃ is the thermal conductivity of the (dry) concrete [35].

The particle surface temperature is given as:

Table 2
Constants and known values used in the model.

Symbol	Description	Approx. value
ρ_c	Density of the dry concrete [kg/m^3]	2000–2200
m	Moisture [%]	6
m_{st}	Mass of steam [kg]	-
m_w	Mass of water [kg]	-
$C_{p,s}$	Heat capacity of steam [J/kg℃]	2000
$C_{p,c}$	Heat capacity of concrete [J/kg℃]	1000
$C_{p,w}$	Heat capacity of water [J/kg℃]	4200
H_{vap}	Heat of vaporization [MJ/kg]	2.26
T_b	Boiling temperature [℃]	100
λ_c	Thermal conductivity of dry concrete [W/m℃]	1.2

$$T_s(t) = T_b + \frac{Q(t)}{4\pi\lambda_c}\left(\frac{1}{R_m(t)} - \frac{1}{R}\right) \tag{3}$$

The cumulative heat absorbed by the particle is:

$$Q_{\text{cum}}(t) = \rho_c \frac{4\pi R^3}{3}\left(C_{p,c} + mC_{p,w}\right)T_b + \rho_c \frac{4\pi}{3}\left(R^3 - R_m^3\right)mH_{\text{vap}} \tag{4}$$

Where, the values of constants used in the model are given in Table 2.

It is proposed that spalling occurs when the tensile strength of the material at some radius of the particle is exceeded by the mechanical stress caused by the thermal expansion of the dry shell of the particle. According to Toshiaki Hata [36], heating a solid sphere of radius R made from a homogeneous material with constant Young's modulus (E) and poisons ratio (ν) to radially symmetrical temperature distribution $T(r,t)$ at a time t produces a displacement (deformation) $u(r,t)$ described by:

$$\frac{1-\nu}{1+\nu}\frac{\partial}{\partial r}\left[\frac{1}{r^2}\frac{\partial}{\partial r}\left(r^2 u\right)\right] = \alpha\frac{\partial T}{\partial r} \tag{5}$$

Where the parameter $\alpha(1/K)$ is the constant linear thermal expansion coefficient of the material. Solutions of this equation are regular at $r = 0$:

$$u(r,t) = \frac{(1-\nu)}{(1+\nu)}\frac{1}{\partial r}\int_0^r \alpha T(r,t)r^2 dr + Ci \tag{6}$$

Ci is a constant determined from boundary conditions. The corresponding radial (σ_r) and tangential (σ_ϑ) stresses for a spherical symmetry are given as:

$$\sigma_r = \frac{E}{(1+\upsilon)(1-2\upsilon)}\left[(1-\upsilon)\frac{\partial u}{\partial r} + 2\upsilon\frac{u}{r} - (1+\upsilon)\alpha T\right] \tag{7}$$

$$\sigma_\vartheta = \frac{E}{(1+\upsilon)(1-2\upsilon)}\left[\upsilon\frac{\partial u}{\partial r} + \frac{u}{r} - (1+\upsilon)\alpha T\right] \tag{8}$$

or, considering that $\sigma_r(R,t) = 0$:

$$\sigma_r = \frac{2E}{3(1-\upsilon)}\left[\overline{X}(R,t) - \overline{X}(r,t)\right] \tag{9}$$

$$\sigma_\vartheta = \frac{E}{3(1-\upsilon)}\left[2\overline{X}(R,t) + \overline{X}(r,t) - 3X(r,t)\right] \tag{10}$$

with $X(r,t)$ representing the expansion with respect to a constant reference temperature, the boiling temperature of moisture is chosen as a reference:

$$X(r,t) = \alpha\left[T(r,t) - T_b\right] \tag{11}$$

The average sign indicates the volume-average of $X(r,t)$ from the centre to radius r:

$$\overline{X}(r,t) = \frac{\int_0^r 4\pi r'^2 \alpha\left[T(r',t) - T_b\right]dr'}{4\pi r^3/3} \tag{12}$$

In order to account also for the effect of radial variations in the moisture concentrations and corresponding volumetric expansion/shrink, we add $\mu[m(r,t) - m_0]$ to the term $\alpha[T(r,t) - T_b]$ in the result by Toshiaki Hata [36]:

$$X(r,t) = \mu\left[m(r,t) - m_0\right] + \alpha\left[T(r,t) - T_b\right] \tag{13}$$

$$\overline{X}(r,t) = \frac{\int_0^r 4\pi r'^2\left\{\mu\left[m(r',t) - m_0\right] + \alpha\left[T(r',t) - T_b\right]\right\}dr'}{4\pi r^3/3} \tag{14}$$

Now, considering a condition where the moisture is instrumental in keeping the core temperature low, while at the same time, the temperature in the dry outer shell increases to the point where the outer shell expands so much that the core breaks loose from the shell as a result of tensile stress. This condition is interesting for industrial applications. The equations of physics also allow other solutions, e.g., where most of the heat is used for heating the dry concrete, or where heating is so slow that all the moisture evaporates without reaching a stress that breaks the particle. The equations derived below may not hold for such limits, but this is not the objective here.

The contribution of temperature fluctuations to the stress term $\overline{X}(r,t)$ is:

$$\overline{X}_T(r,t) = \begin{cases} 0 & 0 < r < R_m \\ \dfrac{\alpha q(t) R^2}{\lambda_c A(t) r}\left(\dfrac{r}{R_m} + \dfrac{R_m^2}{2r^2} - \dfrac{3}{2}\right) & R_m < r < R \end{cases} \tag{15}$$

Including the effect of moisture, it can be rearranged as:

$$\overline{X}(r,t) = \begin{cases} 0 & 0 < r < R_m \\ \dfrac{\alpha q(t) R^2}{\lambda_c A(t) r}\left(\dfrac{r}{R_m} + \dfrac{R_m^2}{2r^2} - \dfrac{3}{2}\right) - \mu m_0\left(1 - \dfrac{R_m^3}{r^3}\right) & R_m < r < R \end{cases} \tag{16}$$

Since $\overline{X}(r,t) = 0$ inside the core, the tensile stress in the core is given by:

$$\sigma = \frac{2E}{3(1-\upsilon)}\overline{X}(R,t) = \frac{2E}{3(1-\upsilon)}\left\{\frac{\alpha q(t) R^2}{\lambda_c A(t) R}\left(\frac{R}{R_m} + \frac{R_m^2}{2R^2} - \frac{3}{2}\right) - \mu m_0\left(1 - \frac{R_m^3}{R^3}\right)\right\}$$

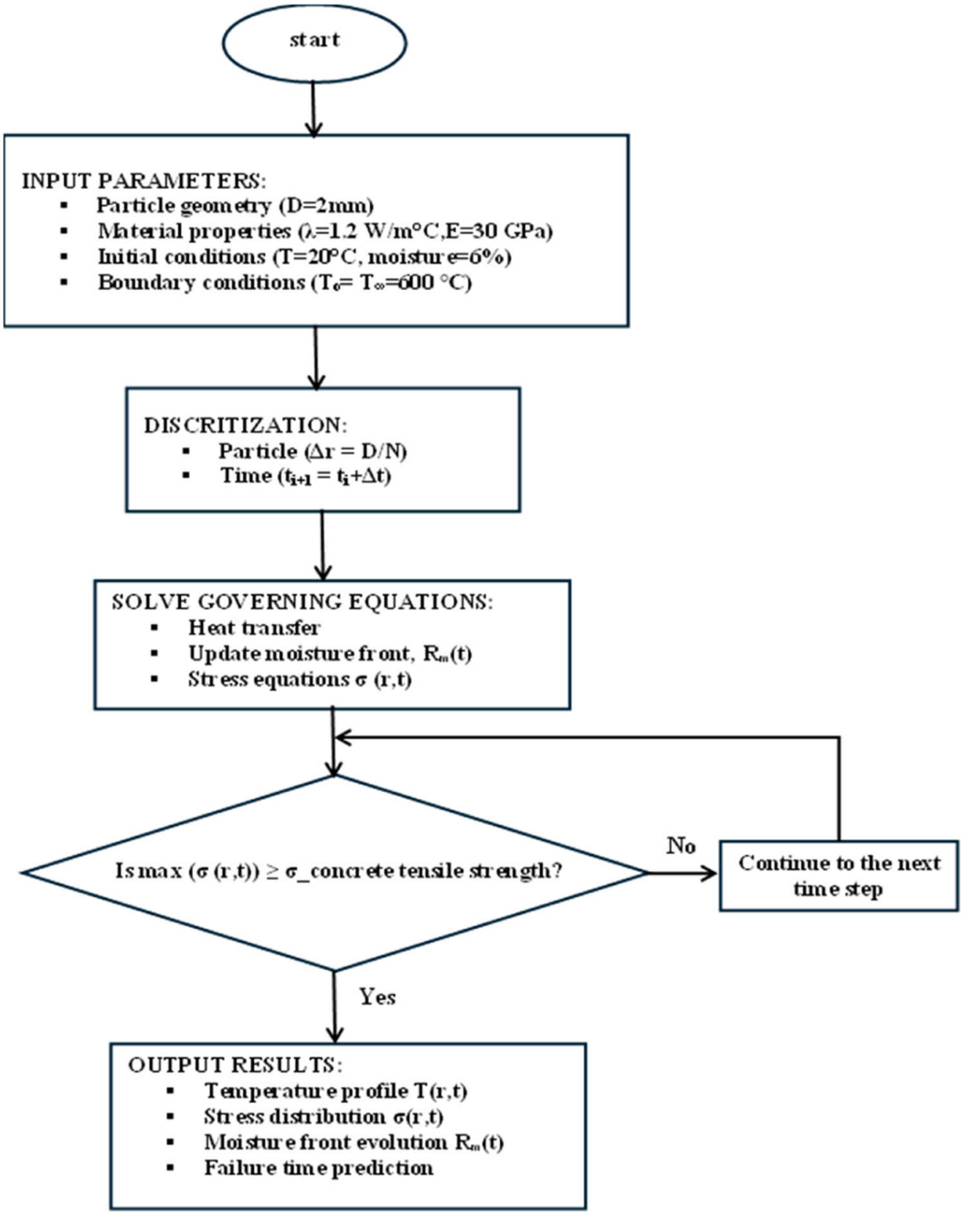

Fig. 4. Flow diagram of 1D thermo-mechanical model for concrete particles under thermal shock.

$$= \frac{2E}{3(1-\upsilon)}\left\{\alpha(T_s(t)-T_b)\left(1-\frac{1}{2}\frac{R_m}{R}\left(1+\frac{R_m}{R}\right)\right)-\mu m_0\left(1-\frac{R_m^3}{R^3}\right)\right\} \tag{17}$$

Finally, $R_m(t)$ needs to be computed as the dry shell increases to the point of spalling. This is governed by the equation given as:

$$m_0\rho_c\Delta H\frac{d}{dt}\left[\frac{4\pi}{3}R_m^3\right] = m_0\rho_c\Delta H4\pi R_m^2\frac{dR_m}{dt} = -4\pi R^2\frac{q(t)}{A(t)} \tag{18}$$

The parameters $\alpha[1/\mathrm{K}]$, $E[\mathrm{Pa}]$ and υ are the linear expansion coefficient, Young's modulus and Poisson's ratio for concrete, respectively. Based on literature data [37,38], the values are given as, $\alpha = 12 \times 10^{-6}$ 1/K, $E =$ 26 GPa and $\nu =$ 0.17. The value for the moisture expansion as a result of moisture content is estimated as, $\mu = 34 \times 10^{-4}$ [39,40].

Thus, the particle will disintegrate or fail when $\sigma_r > \sigma_{\mathrm{concrete}}$ within the core of the particle. The limit $\sigma_{\mathrm{concrete}}$ is a material-dependent parameter, typically representing the tensile strength of a concrete. The literature suggests a value of 2–8 MPa [38,41].

In general, the above one-dimensional thermo-mechanical model provides a framework for predicting the thermal and mechanical response of concrete particles subjected to rapid heating. The transient temperature distribution within the particle is obtained by solving the radial heat conduction equation in spherical coordinates. The flow diagram for the mathematical computation process is shown in Fig. 4.

3. Result and discussion

3.1. 3.1 Baseline study on the property of input RFA

Since the objective of this study is to recover the cement paste embedded within the fine aggregates (0.5 –4 mm), the ultrafine fractions (<0.5 mm) are not included in this study. To understand the initial properties of the input (reference) material, firstly, the physical property and the composition of the reference sample are studied. Under the microscope, most RFA are observed as agglomerates of smaller sand particles glued together by cement paste. This can be seen in Fig. 5 (A). The composition of these aggregates is examined using XRF spectroscopy (PANalystical, epsilon3-XL) after being pulverized into powdered form. The major oxide composition of the input RFA sample is given in Table 3. As can be seen in the table, even though the major composition of these aggregates is silica (SiO_2), a significant amount of CaO and other oxides are still embedded within the aggregates.

When these reference particles are washed with 4 N HCl for about 3 h, most of the cement paste gets dissolved and thus, the sand and other fine aggregates appear to emerge as the real aggregates that had been glued by cement. Fig. 5 (right) shows the microscope image of acid-washed RFAs. Here, it can be assumed that this was the original composition and grain size of the sand fraction.

The PSD of the acid-washed aggregates is then examined by sieving (NEN-EN 933–1) and is shown in Fig. 6.

Based on the PSD of acid washed aggregate samples, recycled aggregates categorized as 2–4 mm, 1–2 mm and 0.5–1 mm are a mix of different sized sand aggregates glued by the hydration products of cement. Thus, for 2–4 mm particles, 52.7 % of the input sample has smaller grains than the initially designated particle size. Similarly, 53.6 % of the 1–2 mm and 35 % of the 0.5–1 mm particles are composed of smaller sand particles that are liberated due to the dissolution of cement paste by acid. It is believed that when recycled particles are exposed to the right thermal conditions, they will disintegrate into similar pieces of sand grains with PSD that resemble the acid-washed particles. Thus, under perfect spalling conditions, the PSD of acid washed particles and thermally treated particles could be assumed similar. In reality, not all recycled fine aggregates are expected to spall completely because optimum thermal conditions may vary depending on the size of particles.

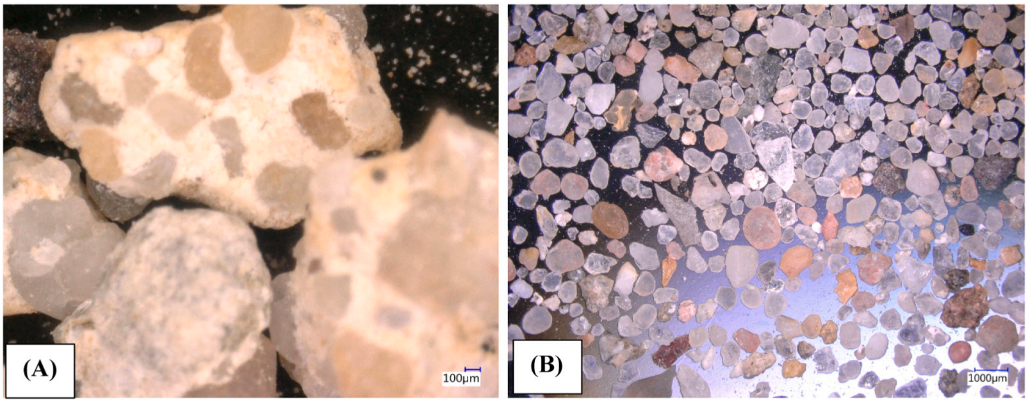

Fig. 5. Optical microscopy image of RFA (A) and the same RFA after being washed with acid (B).

Table 3
Composition of the major oxides for the input RFA reference samples.

Sample	SiO_2	CaO	Al_2O_3	Fe_2O_3	K_2O	SO_3	MgO	Others
0.5–1 mm	74.07	16.15	4.69	2.14	0.92	0.62	0.87	0.54
1–2 mm	70.23	18.5	5.46	2.97	0.94	0.72	1.08	0.1
2–4 mm	68.86	19.2	5.62	3.12	0.92	0.61	1.07	0.6

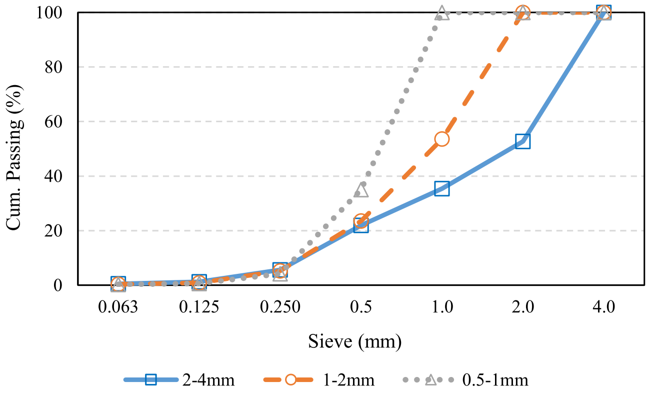

Fig. 6. PSD of recycled fine aggregates (RFA) after being dissolved in an acid.

3.2. *The effect of thermal treatment and subsequent milling of RFAs*

Introducing RFA to thermal shock results in a breakdown of the agglomerates into smaller particles including cement paste powder. In this context, spalling is defined as, “the amount of smaller particles liberated due to disintegration of recycled aggregates as a result of thermal shock.” The newly generated particles have a smaller size than the original particles. Thus, the spalled particles are identified by sieving the samples after each experiment. Those particles passing the smaller sieve are considered spalled particles and their mass ratio is used to quantify the degree of spalling. For instance, for 0.5–1 mm samples, all particles are originally retained at a 0.5 mm sieve. After thermal treatment, 25.2 % of the original sample passes a 0.5 mm sieve and these new particles are obviously generated by the effect of spalling. Similarly, 1–2 mm and 2–4 mm RFA particles display 24 % and 17.2 % spalling, respectively. This shows that the particles get weakened and crackled at the interface between sand and cement paste, generating a different PSD than the reference particles.

Similar phenomenon has been studied by Annerel et al. [2], where the appearance of micro-cracks at the interface between aggregates and cement matrix is observed using polarizing and fluorescence spectroscopy. Since the cement paste matrix is weakened by the thermal shock, further milling helps to complete the liberation of sand and hydrated cement powder. Nevertheless, when process

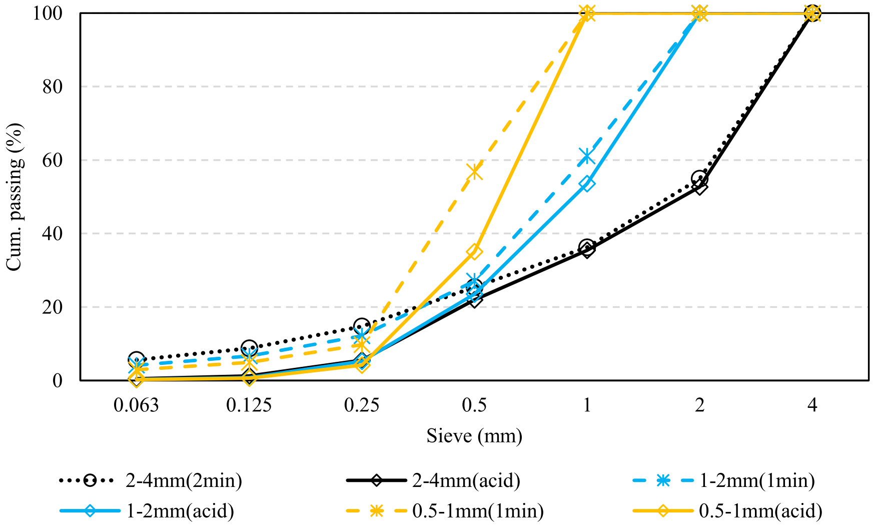

Fig. 7. PSD of processed RFA samples after milling plotted along with the PSD of the acid-washed input.

conditions like residence time and temperature are not controlled, the ultimate consequence of spalling could be detrimental and as a result, the aggregate itself may suffer fracture and crack due to extensive thermal expansion, making the property of recovered sand weaker. Thus, control over residence time has paramount importance.

By applying a gentle milling using smaller steel balls of diameter 8–12 mm and maintaining a sample to milling ball ratio of 1:5, it is possible to liberate most cement paste from the aggregate surface. Fig. 7 displays PSD of milled RFA after being exposed to thermal shock. As shown in the figure, milling of these particles generates more Recycled Cement-rich Powder (RCP). By comparing the PSD of milled particles with that of acid-treated particles, it is possible to tell the similarity in PSD curves between milled and acid-washed samples. This comparison is important because the similarity of PSD curves suggests that most cement paste has been liberated from the surface of particles. Indeed, different sized RFAs may favor different milling times. As shown in Fig. 7, larger fractions (2–4 mm) favor 2 min of milling time. Similarly, 1 min milling time is preferred for both 1–2 mm and 0.5–1 mm particles. This would enable to recover 6–10 % of the attached cement from recycled sand grains excluding the amount of cement paste recovered during preliminary crushing. The powdered fraction (<0.125 mm) generated due to milling is rich in CaO. The composition of this product resembles cement paste than the aggregate.

The composition of each particle size is determined by pulverizing particles on each sieve and the oxide composition is analyzed by XRF. The implication of this experiment is to make a simple comparison in the amount of CaO (and SiO_2) which may help to understand the liberation of cement paste from the aggregate particles. As we process RFA the amount of CaO drops, and the aggregates become clean and rich in SiO_2. This evidence verifies that a combination of thermal shock with gentle milling is a good combination for liberating and cleaning the cement paste from the surface of fine aggregates.

Table 4 shows the oxide composition of fine aggregates before and after processing. It is evident that as the RFA sample is processed, the amount of CaO decreases, while the amount of SiO_2 increases across all cases. For instance, for 0.5–1 mm samples, the amount of CaO decreases from 16.15 % to 4.34 %, and similarly the amount of SiO_2 increases from 74.07 % to 90.03 % which may be interpreted as the liberation of cement paste from the surface of the fine aggregate. The same trend is observed in the other test cases.

On the other hand, the composition of RCP has been analyzed and is found to be rich in calcium oxide (CaO) and silica (SiO_2). This fraction has the potential to replace part of cement in the production of concrete. Several studies suggest that such cement-rich powder can be used to partially replace cement in a mortar without compromising its strength [42,43]. This study also confirms an optimum replacement level of 15 %. However, achieving a high level of replacement may necessitate additional processing of the powder, such as high-temperature treatment accompanied by milling, to enhance its properties. Nonetheless, utilizing RCP as an alternative raw material in the production of cement presents a viable and practical solution [29]. A comparative comparison in oxide composition of RCP and CEMIII is given in Table 5. The composition of RCP clearly differs from that of cement, particularly in its calcium oxide (CaO) and silicon dioxide (SiO_2) content. The high silica levels may be attributed to the milling process.

3.3. Performance of RCP in mortar

Since the objective of this test is to evaluate the reusability potential of RCP recovered through thermal shock, the consistency of the mortar has been kept similar for all mixes by adjusting the workability with water. For this, extra 5 %, 9 % and 13 % additional mixing water is utilized for RCP-10, RCP-15 and RCP-20, respectively. The water absorption of RCP is usually higher than that of conventional cement [21,44]. This higher absorption capacity means that RCP particles absorb a portion of the mixing water during the preparation of mortar, reducing the amount available for cement hydration and lubrication of the mix. In mortar mix design, this necessitates adjustments to maintain desired workability. Adding more water to compensate for RCP's absorption directly influences strength development by increasing the effective water-to-cement (w/c) ratio, which may dilute the cement paste and create excess pores during hydration [20]. This could lead to reduced compressive strength. As shown in Fig. 8, the compressive strength results indicate that a 15 % substitution of RCP yields the most favorable performance, demonstrating higher early-age strength and comparable 28-day strength relative to the reference mix (Ref). Interestingly, both the 10 % and 20 % RCP mixes exhibited lower strengths (and higher standard deviations), making the performance peak at 15 % substitution particularly notable. While the exact mechanism remains unclear, this enhancement could be attributed to either accelerated hydration kinetics or a reactive filler effect from the RCP particles. However, the composition of RCP shown in Table 5 tells the potential of the RCP and the need for further processing to render the required reactivity to achieve higher rates of cement substitution. Enhancing the composition and morphology of RCP and optimizing its replacement level in mixes could result in a more sustainable construction material with improved mechanical properties.

3.4. Modelling study

The model, in general, tries to predict the particle temperature history and residence time necessary to weaken and fracture the fine

Table 4
The average composition of the RFA before and after thermal processing and milling.

Sample	**0.5–1 mm**		**1–2 mm**		**2–4 mm**	
	SiO_2	CaO	SiO_2	CaO	SiO_2	CaO
Input RFA (Reference)	74.07	16.15	70.23	18.5	68.86	19.2
Thermal Processed RFA	78	12.5	72.53	16.11	71.59	17.16
Thermal Processed RFA + milled	90.03	4.34	83.67	7.3	76.12	12.83

Table 5
The composition of RCP compared to CEM III.

Sample	SiO_2	CaO	SO_3	Fe_2O_3	Al_2O_3	K_2O	MgO	Cl^-	Others	LOI
RCP	50	32	4.7	3.9	4.16	1.03	0.85	0.05	0.21	3.1
CEM III/A 42.5	26	51.9	3.2	3	7.7	0.8	4.6	0.007	0.8	2

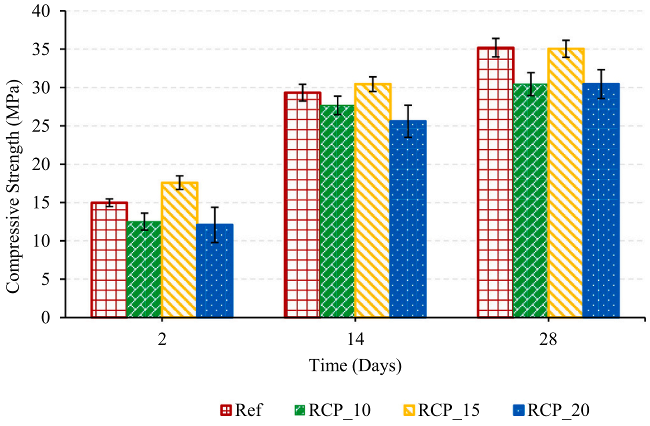

Fig. 8. Strength development of a mortar made at different substitution rates of RCP.

aggregates during thermal exposure. It also shows the distribution of internal stress inside the particle as a function of time. The application of such model is significant for designing an industrial process that can be used to thermally treat recycled fine aggregates and be able to separate into clean recycled sand and cement-rich powder.

When concrete is subjected to temperatures higher than 100 °C, the differential strain between the centre and the outer shell which often shrinks, will initially induce a small compressive stress in the core [22]. As the temperature increases, the compressive stress becomes insignificant and tensile stress becomes a more dominant force. Based on the literature [2,45], at temperatures above 105 °C, evaporation and dehydration (i.e. release of chemically bound water) from the C-S-H become significant and at 350 °C dissociation of ettringite is apparent and as a result, visible interfacial cracks are observed. According to the model, this phenomenon is clearly shown in Fig. 9 where the shrinkage of the matrix is displayed as negative stress. As the temperature progresses, expansion of the matrix dominates and is shown as positive stress in the figure. When the radial stress outweighs the tensile strength of the concrete, the particle is weakened and ultimately fails (spalled). The peak indicated in Fig. 9 is an indication of the average time needed for 2 mm particles to get spalled when exposed to a processing temperature of 600 °C. The particle temperature history also shows that the particle's surface heats quickly and the moisture escapes easily from the surface. However, the heat flow encounters resistance to diffuse into the particle. This resistance builds a gradient in temperature between the core and surface causing the particle to react in terms of crackling, weakening, or spalling.

Sensitivity analysis on the model shows that the processing temperature and residence time are directly related. Fig. 10 shows the relationships between processing temperature and residence time. The higher the processing temperature, the lower the residence time and vice versa. This means, when the particle is subjected to higher temperature, it experiences thermal shock, leading to quicker

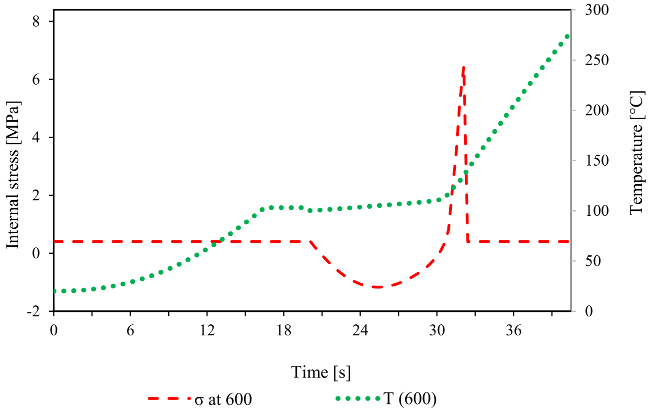

Fig. 9. Temperature and internal stress for 2 mm concrete particle at a processing temperature of 600 °C.

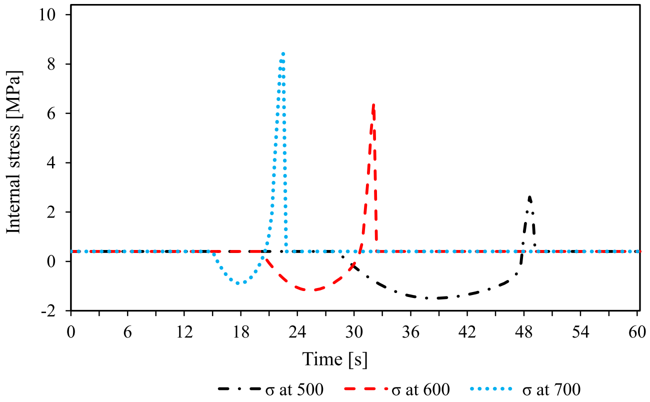

Fig. 10. Sensitivity of radial stress (σ) at different processing temperatures for 2 mm concrete particles.

spallation. This is due to the big gradient in temperature established between the fast-heating particle surface and the wet internal core. Thus, when a 2 mm aggregate particle is exposed to processing temperatures of 500 °C, 600 °C and 700 °C, it spalls at 49, 33 and 22 s, respectively.

3.5. Model validation

Validation of the model is done in two ways. Firstly, based on the model prediction, a residence time of 33 s is chosen for 2–4 mm particles. Thus, 2–4 mm particles are exposed to 600 °C for 33 s in an oven and then gently milled for 2 min. When the PSD of these samples is compared with the acid-washed samples, the resemblance in their PSD is used to verify the prediction of the model. Fig. 11 (A) compares the PSD of particles after heating in an oven for 33 s and milled samples (33 +mill). Based on this graph, 2–4 mm particles generate a PSD that closely matches the PSD of acid-washed samples that are assumed to represent perfectly liberated particles. This validates the predicted residence time of 33 s for 2–4 mm particles, suggesting effective removal of cement paste.

Secondly, the predicted particle temperature from the thermal model is validated by a series of controlled experiments in an oven. Validation experiments are carried out by heating 2–4 mm particles in an oven at different residence times (10, 20, 30 and 35 s). The surface temperature of the particles was measured using a calibrated infrared thermometer. The experimental surface temperatures are compared to the model-predicted values. The comparison showed good agreement within the expected measurement uncertainty, confirming that the model reliably captures the thermal response of small particles under high-temperature exposure. Fig. 11(B) shows the Temperature versus residence time predicted by the model and experimental results. As shown in the figure, the experimental and model results are in good agreement.

Practically, RFA have a particle size range of 0–4 mm and are often processed all together. The fact that these experiments are performed at a specific size range and the model being implemented for a single particle size, may suffer some limitations. While the 1D model simplifies the analysis, complex phenomenon may not be captured properly during rapid heating. Besides, the assumption of homogeneity in the Toshiaki Hata model [36] may lead to an underestimation of the spalling time. Consequently, concrete being a heterogeneous material, little deviations are expected from the model prediction. Overall, the results conveyed from this study are a step forward in developing recycling technologies that would enable to reclaim high-quality recycled sand and cement-rich powder in an economical and cost-effective way. Taking the inputs from both experimental and model results into consideration, a pilot scale thermal recycling unit with a capacity of 10 t/h has been designed adn this has been patented under US 2021/0107831A1[46]. The implementation of process parameters into the newly designed HAS setup is a successful application of experiments and the model.

3.6. Economic and environmental feasibility

This study represents a proof of concept on the thermo-mechanical recycling of cement-rich powder. It is based on the assumption that recycled cement-rich powder (CRP) could be valorized as a supplementary cementitious material (SCM) or as a filler in blended binders. This partial substitution reduces demand for Portland cement clinker, leading to indirect CO_2 and cost savings. Moreover, because the method upgrades a waste fraction (RFA) that currently has low-value applications, it adds a potential revenue stream. A more detailed techno-economic and life-cycle assessment will be required in future work, but initial indications suggest that the reduced energy demand and resource recovery provide a promising balance between environmental and economic performance.

The thermo-mechanical recycling of cement-rich powder involves energy costs for heating and grinding. The economic viability of the approach is also supported by the potential for lower overall costs compared to traditional methods that involve heating for longer residence times [25]. To give an overview of the economic analysis, let's base our calculation on the amount of energy required for the process, which is the sum of energy required for thermal shock and the energy required for milling or grinding the fines. Energy required for thermal shock can be calculated based on the following formula,

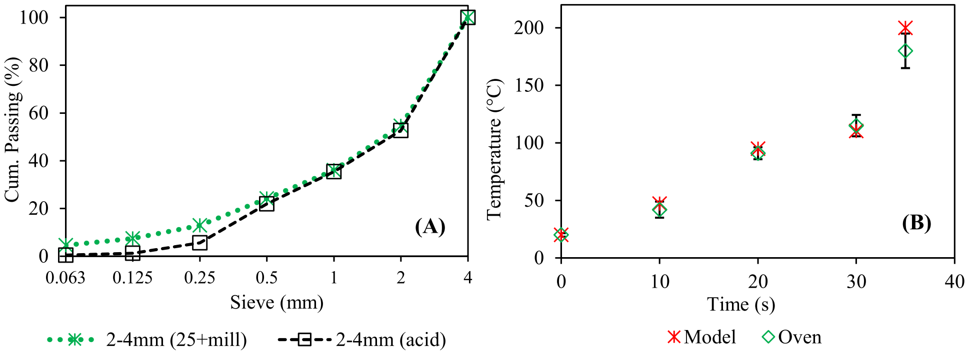

Fig. 11. PSD of spalled and milled 2–4 mm RFA particles compared to acid washed particles (A); and validation of particle surface temperature with experiments (B).

$$Q_{duty} = \left[m_W C_{pw} \Delta T\right] + \left[m \Delta H_v\right] + \left[m_{st} C_{Ps} \Delta T\right] + \left[m_s C p_s \Delta T\right] \tag{19}$$

where the first term $(m_w C_{pw} \Delta T)$ indicates the amount of energy needed to raise the temperature of moisture from room temperature to boiling temperature (T_b), the second term refers to heat of vaporization $[m \Delta H_v]$, the third term is to carry the steam $[m_{st} C_{Ps} \Delta T]$ and the last term is the amount of heat energy absorbed by the solid particles $[m_s C p_s \Delta T]$. The nomenclature and value of constants is introduced in Table 2.

Thus, the amount of energy required for thermal shock is 90 kW per ton of input materials (which is 0.09 kWh/kg) and the energy required for laboratory milling device is about 0.16 kWh/kg. This gives the total energy required for the process to be roughly around 0.25 kWh/kg. In comparison, conventional Portland cement production consumes roughly 0.9 –1.1 kWh/kg; where the thermal energy required for clinker production (0.8–1.0 kWh/kg) and electrical energy for grinding is 0.1–0.12kWh/kg [47–49]. Thus, RCP recovery requires about one-fourth of the energy of cement production. From an environmental perspective, producing Portland cement emits ~0.8–0.9 kg CO_2/kg, mainly from limestone calcination [49]. In contrast, RCP recovery emits only ~0.2 kg CO_2/kg primarily from the type of fuel used, representing a potential reduction of up to 65 % in carbon footprint. This highlights the energy and carbon saving of valorizing RCP as a supplementary cementitious material. However, it is necessary to be cautious about the following factors when carrying out a comprehensive cost-benefit analysis:

- If diesel is used for drying or pre-drying samples, the advantage shrinks.
- Lab thermal-shock experiments can be inefficient at scale. Heat losses and low throughput, increase energy per kg. Conversely, optimized industrial designs can greatly reduce per-kg energy.
- Laboratory ball-milling numbers are mostly higher than industrial milling; energy depends on target fineness, mill type, and throughput.
- RCP typically has limited hydraulic performance compared to Portland cement. The net CO_2 benefit depends on how much RCP can replace cement in applications. If RCP is further carbonated to store CO_2, it could have significant carbon saving potential.

4. Conclusion

Thermal shock is a means by which particles disintegrate when exposed to high temperatures. This method is applied to recycle the fine fraction of recycled aggregates, which are often sidelined during recycling activities and frequently downcycled as road base material or landfilled. This study is supported by extensive experiments and model prediction. The study reveals the possibility of turning Recycled Fine Aggregates (RFA) into clean fine aggregates (recycled sand) and hydrated cement-rich powder by using thermo-mechanical treatment methods. This is a step forward in recycling end-of-life concrete wastes and helps to close the materials loop in the construction sector and improve circularity of resources. The main conclusions drawn from this study are:

- When fine recycled aggregates are exposed to quick heat flow rates, the surface heats quicker than it conducts to the inner particle and it creates a gradient in temperature. This gradient is the driving factor for spalling or disintegration of aggregates that have been held together by the cement paste. Based on this study, at a processing temperature of 600 ℃, an average residence time of 30–40 s is enough for recovering much of the RCP from RFA. Further milling of the heat-treated particles for a maximum of 2 min completes recovery of clean sand and hydrated cement-rich powder from the fine recycled aggregates. Besides, milling increases the quality and quantity of recycled cement-rich powder. This method increases the amount of recoverable cement-rich powder (RCP), but it does not appear to significantly reactivate its hydraulic properties.
- A particle model has been developed to understand the stress-related phenomena during thermal treatment. The model is able to predict the residence time where a particle spalls/weakens upon exposure to a specific processing temperature. In this case, 600 ℃, 33 s, and 2-minute milling time are considered suitable process variables for recycling at industrial scale. The model has been validated by experimental results.

- As thermal spalling can have a detrimental effect on the final property of aggregates, control over the temperature and residence time is essential. On the other hand, high process temperatures could be advantageous for dehydration of RCP.
- The compressive strength results indicate that a 15 % substitution of RCP yields the most favorable performance, demonstrating higher early-age strength and comparable 28-day strength relative to the reference mix (Ref). While the exact mechanism remains unclear, this enhancement could be attributed to either accelerated hydration kinetics or a reactive filler effect from the RCP particles. Further investigations are recommended to determine whether the early strength gain is driven by supplementary cementitious material (SCM) reactivity or by physical characteristics like particle packing or filler action.
- In conclusion, this research identifies significant variables that may help develop a thermo-mechanical technology that utilizes thermal shock, milling, and classification methods to reclaim cement-rich powder and recycled sand from RFA. Further study on the characteristics and properties of recycled sand and in-depth analysis on recycled cement-rich powder will be conducted in the future.

CRediT authorship contribution statement

Cheng Chang: Writing – review & editing, Validation, Resources. **Francesco Di Maio:** Writing – review & editing, Resources, Project administration, Formal analysis, Conceptualization. **Peter Rem:** Writing – review & editing, Visualization, Validation, Supervision, Methodology, Formal analysis, Conceptualization. **Ali Vahidi:** Writing – review & editing, Visualization, Validation, Resources, Methodology, Formal analysis. **Gebremariam Abraham Teklay:** Writing – review & editing, Writing – original draft, Visualization, Validation, Resources, Methodology, Investigation, Conceptualization.

Declaration of Competing Interest

The authors declare the following financial interests/personal relationships which may be considered as potential competing interests: Peter Rem has patent #US 2021/0107831A1 licensed to C2CA Technology BV. If there are other authors, they declare that they have no known competing financial interests or personal relationships that could have appeared to influence the work reported in this paper.

Acknowledgement

The authors acknowledge the financial support from EU Horizon 2020 Project ICEBERG "Innovative Circular Economy Based solutions demonstrating the Efficient Recovery of valuable material resources from the Generation of representative end-of-life building materials" (No. 869336).

Data availability

Data will be made available on request.

References

[1] M. Malešev, V. Radonjanin, S. Marinković, Recycled concrete as aggregate for structural concrete production, Sustainability 2 (2010) 1204–1225, https://doi.org/10.3390/su2051204.

[2] E. Annerel, L. Taerwe, Assessment of the fire damage of concrete members after fire exposure, in: M. Fardis (Ed.), Innovative Materials and Techniques in Concrete Construction, Springer, Dordrecht, 2012, https://doi.org/10.1007/978-94-007-1997-2.

[3] A.G. Razaqpur, G. Fathifazl, B. Isgor, A. Abbas, B. Fournier, S. Foo, How to produce high quality concrete mixes with recycled concrete aggregate, 2nd Int. Conf. Waste Eng. Manag. ICWEM 2010. 73 (2010) 11–35.

[4] Z. Shui, D. Xuan, H. Wan, B. Cao, Rehydration reactivity of recycled mortar from concrete waste experienced to thermal treatment, Constr. Build. Mater. 22 (2008) 1723–1729, https://doi.org/10.1016/j.conbuildmat.2007.05.012.

[5] D. Gastaldi, F. Canonico, L. Capelli, L. Buzzi, E. Boccaleri, S. Irico, An investigation on the recycling of hydrated cement from concrete demolition waste, Cem. Concr. Compos. 61 (2015) 29–35, https://doi.org/10.1016/j.cemconcomp.2015.04.010.

[6] A. Mohammadinia, A. Arulrajah, M.M. Disfani, S. Darmawan, Small-Strain behavior of Cement-Stabilized recycled concrete aggregate in pavement base layers, J. Mater. Civ. Eng. 31 (2019) 1–13, https://doi.org/10.1061/(ASCE)MT.1943-5533.0002671.

[7] C.S. Poon, D. Chan, Feasible use of recycled concrete aggregates and crushed clay brick as unbound road sub-base, Constr. Build. Mater. 20 (2006) 578–585, https://doi.org/10.1016/J.conbuildmat.2005.01.045.

[8] United nations environment programme, sand, rarer than one thinks, Environ. Dev. 11 (2014) 208–218, https://doi.org/10.1016/j.envdev.2014.04.001.

[9] M. Bendixen, J. Best, C. Hackney, L.L. Iversen, Time is running out for sand, Nature 571 (2019) 29–31, https://doi.org/10.1038/d41586-019-02042-4.

[10] Roadmap Hergebruik Betonreststromen, Utrecht, Netherlands, 2021. ⟨https://www.betonakkoord.nl/resultaten/⟩.

[11] A.T. Gebremariam, F. Di Maio, A. Vahidi, P. Rem, Innovative technologies for recycling End-of-Life concrete waste in the built environment, Resour. Conserv. Recycl 163 (2020) 104911, https://doi.org/10.1016/j.resconrec.2020.104911.

[12] A. Carriço, J.A. Bogas, S. Hu, S. Real, M.F. Costa Pereira, Novel separation process for obtaining recycled cement and high-quality recycled sand from waste hardened concrete, J. Clean. Prod. 309 (2021), https://doi.org/10.1016/j.jclepro.2021.127375.

[13] M.V.A. Florea, Z. Ning, H.J.H. Brouwers, Smart crushing of concrete and activation of liberated concrete fines, Eindhoven, 2013. ⟨https://slimbreker.nl/downloads/SC1⟩ Final Report.pdf, Accessed on July, 2019.

[14] R.S. Bogas, J., M. Pereira, A. Guedes, A. Carriço, S. Hu, Separation process of waste hardened concrete for obtaining recycled cement from waste concrete, International patent application PCT/PT2021/050005 (2020) priority date 23/02/2021, 2020.

[15] E. Pawluczuk, K. Kalinowska-Wichrowska, M. Bołtryk, J.R. Jiménez, J.M. Fernández, The influence of heat and mechanical treatment of concrete rubble on the properties of recycled aggregate concrete, Materials 12 (2019), https://doi.org/10.3390/ma12030367.

[16] R. Prajapati, R. Gettu, S. Singh, Thermomechanical beneficiation of recycled concrete aggregates (RCA), Constr. Build. Mater. 310 (2021) 125200, https://doi.org/10.1016/j.conbuildmat.2021.125200.

[17] H. Shima, H. Tateyashiki, R. Matsuhashi, Y. Yoshida, An advanced concrete recycling technology and its applicability assessment through input-output analysis, J. Adv. Concr. Technol. 3 (2005) 53–67, https://doi.org/10.3151/jact.3.53.

[18] L. Xu, J. Wang, K. Li, S. Lin, M. Li, T. Hao, Z. Ling, D. Xiang, T. Wang, A systematic review of factors affecting properties of thermal-activated recycled cement, Resour. Conserv. Recycl. 185 (2022), https://doi.org/10.1016/j.resconrec.2022.106432.

[19] E.A. Ohemeng, S.O. Ekolu, A review on the reactivation of hardened cement paste and treatment of recycled aggregates, Mag. Concr. Res. 72 (2020) 526–539, https://doi.org/10.1680/jmacr.18.00452.

[20] T. Meng, Y. Hong, K. Ying, Z. Wang, Comparison of technical properties of cement pastes with different activated recycled powder from construction and demolition waste, Cem. Concr. Compos. 120 (2021) 104065, https://doi.org/10.1016/j.cemconcomp.2021.104065.

[21] J.A. Bogas, A. Carriço, A.J. Tenza-Abril, Microstructure of thermoactivated recycled cement pastes, Cem. Concr. Res. 138 (2020), https://doi.org/10.1016/j.cemconres.2020.106226.

[22] Y.F. Fu, Y.L. Wong, C.A. Tang, C.S. Poon, Thermal induced stress and associated cracking in cement-based composite at elevated temperatures - part II: thermal cracking around multiple inclusions, Cem. Concr. Compos. 26 (2004) 113–126, https://doi.org/10.1016/S0958-9465(03)00087-8.

[23] D. Gawin, F. Pesavento, B.A. Schrefler, Towards prediction of the thermal spalling risk through a multi-phase porous media model of concrete, Comput. Methods Appl. Mech. Eng. 195 (2006) 5707–5729, https://doi.org/10.1016/j.cma.2005.10.021.

[24] A. Carriço, J.A. Bogas, M. Guedes, Thermoactivated cementitious materials – a review, Constr. Build. Mater. 250 (2020), https://doi.org/10.1016/j.conbuildmat.2020.118873.

[25] S. Gupta, H. Agrawal, S. Chaudhary, Thermo-mechanical treatment as an upcycling strategy for mixed recycled aggregate, Constr. Build. Mater. 398 (2023) 132471, https://doi.org/10.1016/j.conbuildmat.2023.132471.

[26] C. Bu, B. Tan, Q. Wu, Y. Qiao, Y. Sun, L. Yu, Q. Yang, Activation method and reuse of waste concrete Powder-A review, Sustainability 15 (2023), https://doi.org/10.3390/su15065451.

[27] C. Alonso, L. Fernandez, Dehydration and rehydration processes of cement paste exposed to high temperature environments, J. Mater. Sci. 39 (2004) 3015–3024, https://doi.org/10.1023/B:JMSC.0000025827.65956.18.

[28] G.F. Peng, S.Y.N. Chan, M. Anson, Chemical kinetics of C-S-H decomposition in hardened cement paste subjected to elevated temperatures up to 800°C, Adv. Cem. Res. 13 (2001) 47–52, https://doi.org/10.1680/adcr.2001.13.2.47.

[29] J. Schoon, K. De Buysser, I. Van Driessche, N. De Belie, Fines extracted from recycled concrete as alternative raw material for portland cement clinker production, Cem. Concr. Compos. 58 (2015) 70–80, https://doi.org/10.1016/j.cemconcomp.2015.01.003.

[30] M.S. de Juan, P.A. Gutiérrez, Study on the influence of attached mortar content on the properties of recycled concrete aggregate, Constr. Build. Mater. 23 (2009) 872–877, https://doi.org/10.1016/j.conbuildmat.2008.04.012.

[31] A. Akbarnezhad, K.C.G. Ong, M.H. Zhang, C.T. Tam, Acid treatment technique for determining the mortar content of recycled concrete aggregates, J. Test. Eval. 41 (2013) 20120026, https://doi.org/10.1520/jte20120026.

[32] H. Yang, Y. Che, F. Leng, Calcium leaching behavior of cementitious materials in hydrochloric acid solution, Sci. Rep. 8 (2018) 1–9, https://doi.org/10.1038/s41598-018-27255-x.

[33] Yunus A. Cengel, Afshin J. Ghajar. Heat and Mass Transfer: Fundamentals and Applications, 5th ed., Mc Graw Hill, New York, 2015.

[34] Frank P. Incropera, David P. Dewitt, Theodore L. Bergman, Adrienne S. Lavine. Fundamentals of Heat and Mass Transfer, 6th ed., John Wiley & Sons, USA, 2007.

[35] R. Jansson, Fire Spalling of Concrete: Theoretical and Experimental Studies Fire Spalling of Concrete Theoretical and Experimental Studies, KTH, 2013.

[36] T. Hata, Thermal shock in a hollow sphere caused by rapid uniform heating, J. Appl. Mech. Trans. ASME 58 (1991) 64–69, https://doi.org/10.1115/1.2897180.

[37] A. Al-Ostaz, The Effect of moisture on the coefficient of thermal expansion of concrete, Mississippi, 2007.

[38] O. Bahr, P. Schaumann, B. Bollen, J. Bracke, Young's modulus and Poisson's ratio of concrete at high temperatures: experimental investigations, Mater. Des. 45 (2013) 421–429, https://doi.org/10.1016/j.matdes.2012.07.070.

[39] Y. Huang, B. Yuan, L. Xiao, Y. Liu, Studies on the wet expansion deformation of hydraulic concrete with Fly ash under non-standard temperatures, Case Stud. Constr. Mater. 8 (2018) 392–400, https://doi.org/10.1016/j.cscm.2018.03.003.

[40] G.D. Alungbe, Coefficient of Thermal and Moisture Expansion of Concrete Used in Florida, PhD thesis, University of Florida, 1989.

[41] A.M. Neville, J.J. Brooks, Concrete Technology, second Ed., London, 2010. https://doi.org/10.1016/0360-1323(76)90009-3.

[42] Z. Li, Y. Bian, J. Zhao, Y. Wang, Z. Yuan, Recycled concrete fine powder (RFP) as cement partial replacement: influences on the physical properties, hydration characteristics, and microstructure of blended cement, J. Build. Eng. 62 (2022) 105326, https://doi.org/10.1016/j.jobe.2022.105326.

[43] J. Topič, Z. Prošek, T. Plachý, Influence of increasing amount of recycled concrete powder on mechanical properties of cement paste, IOP Conf. Ser. Mater. Sci. Eng. 236 (2017), https://doi.org/10.1088/1757-899X/236/1/012094.

[44] P. Vashistha, Y. Oinam, H.K. Kim, S. Pyo, Effect of thermo-mechanical activation of waste concrete powder (WCP) on the characteristics of cement mixtures, Constr. Build. Mater. 362 (2023) 129713, https://doi.org/10.1016/j.conbuildmat.2022.129713.

[45] M. Castellote, C. Alonso, C. Andrade, X. Turrillas, J. Campo, Composition and microstructural changes of cement pastes upon heating, as studied by neutron diffraction, Cem. Concr. Res. 34 (2004) 1633–1644, https://doi.org/10.1016/S0008-8846(03)00229-1.

[46] H.F. Peter Rem, Peter Berkhout, Jaap Heijboer, Cement waste recycling device and Method of recycling cement waste, US 2021/0107831A1, 2021.

[47] M. Schneider, M. Romer, M. Tschudin, H. Bolio, Sustainable cement production-present and future, Cem. Concr. Res. 41 (2011) 642–650, https://doi.org/10.1016/j.cemconres.2011.03.019.

[48] M. Schneider, V. Hoenig, J. Ruppert, J. Rickert, The cement plant of tomorrow, Cem. Concr. Res. 173 (2023), https://doi.org/10.1016/j.cemconres.2023.107290.

[49] E. Worrell, N. Martin, L. Price, Potentials for energy efficiency improvement in the US cement industry, Energy 25 (2000) 1189–1214, https://doi.org/10.1016/S0360-5442(00)00042-6.